

# Report on the November 2023 ERT survey of Wogan Cavern (Pembroke, Pembrokeshire)

M. Bates & R. Dinnis, 3<sup>rd</sup> April 2024

## Contents

Summary .....	1
November 2023 Electrical Resistivity Tomography (ERT) survey .....	2
Method and application at Wogan Cavern .....	2
Results and interpretation .....	5
East-West transect .....	5
North-South transect.....	5
Concluding comments and future work.....	7
References .....	7
Appendix 1: ERT transects location data by EDM point ID.....	8

## Summary

An Electrical Resistivity Tomography (ERT) survey was undertaken at Wogan Cavern in November 2023, comprising two survey lines – one east-west across the cave, and one north-south from the cave entrance to the cave rear. Although confident interpretation is not possible, the resulting data shows patterning that in part can reasonably be related to known features of the site. The work shows the applicability of geophysics to the site. Further geophysical survey work would therefore be beneficial.

## November 2023 Electrical Resistivity Tomography (ERT) survey

An Electrical Resistivity Tomography (ERT) survey was undertaken at Wogan Cavern by MB and RD on 14<sup>th</sup> and 15<sup>th</sup> November.

### Method and application at Wogan Cavern

ERT survey measures changes in ground resistivity by directly applying an electrical current to the ground. Two metallic spikes are placed into the ground and an electrical current applied across them. Two additional metallic spikes are generally used to measure the potential drop between the current electrodes. The current and potential are then used to calculate the apparent resistivity of the ground. By making a number of measurements at different electrode spacings it is possible to measure the apparent resistivity to different depths within the ground. Traditionally this is done for a number of spacing-depth measurements and these are then interpreted using geo-electrical models of the ground in terms of a true depth-resistivity sounding. In its simplest application, the method assumes a layered earth model. With modern resistivity surveying equipment many electrodes are deployed at a time, and computer control is used to select different electrode pairs for the current and potential electrodes. The result of this type of survey is an apparent resistivity section which again can be modelled in terms of a geo-electrical cross-section or image of the earth for interpretation in terms of sub-surface geology and hydrology. Resolution of subsurface layers with this technique is determined by the electrode spacing, the geometry of current-potential pairs and the resistivity-depth section itself. In general, the deeper in the section, the poorer the resolution, as this requires the use of electrode pairs that are more widely separated and thus more lateral changes in sub-surface geology might be present.

At Wogan Cavern, the electrical imaging collected was acquired using an ABEM Terrameter SAS4000 resistivity meter with 80 electrodes (Fig. 1). Two transects were positioned perpendicular to each other (Fig. 2):

1. An east-west transect (Line LR00028), which ran c.25cm south of the previously excavated part of Trench 9 (i.e. just south of Squares 4 and 7) in the west to c.55cm north of the excavated part of Trench 5 (i.e. the line ran through the unexcavated Squares 3 and 5) in the east (see Dinnis & French 2023).
2. A north-south transect (Line LR00029), which ran from roughly the middle of the grille at the cave mouth in the north to the rear cave wall in the south, passing to the west of the previously excavated part of Trench 8 (i.e. just west of Square 4) (see Dinnis 2023).

The electrode spacing was set to two different separations: Line LR00028 was surveyed at 20cm spacing whereas Line LR00029 was surveyed at 30cm intervals to increase penetration depth.

The position of the transects was chosen to incorporate areas of known intact sedimentary deposits (i.e. those in the areas of Trenches 5 and 9) as well as the area close to Trench 8, which is known to be formed of a significant volume of historical-age disturbance (Dinnis & French 2023; Dinnis 2023). The ERT lines were plotted using an EDM with reference to the local grid used during the 2021-23 excavations. This data is given in Appendix 1.

The ERT data was downloaded from the field instrument using ABEM Terrameter Toolkit and stored as .DAT files which are ASCII text editable. These files were edited to include topographic information in the form of heights relative to OSGB and distances along each line. The lines were surveyed for X,Y with respect to OSGB. Data was then uploaded to Res2dinv for further processing. This included inversion of the data and forward modelling using a smoothness constrained least-squares method (Loke et al. 2003). Goodness to fit for each inversion was accepted when errors were less than 5% between the model data and the survey data. Export from Res2dinv included ERT cross sections as images.



*Figure 1: Looking east along ERT Line LR00028 (east-west transect).*

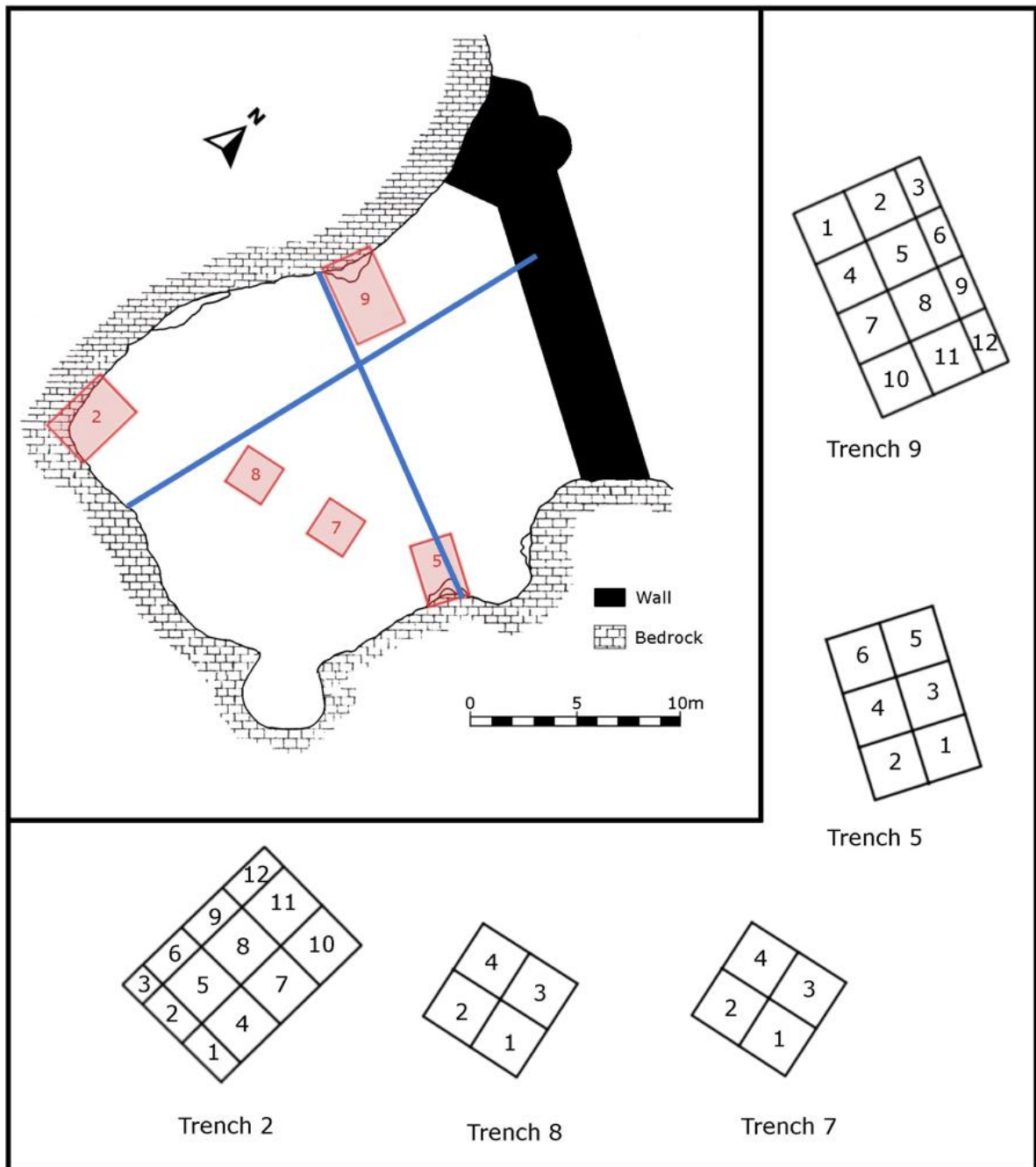


Figure 2: Plan of Wogan Cavern (modified from King 1978: 111), showing the location of the trenches so far tested during the 2021-23 field seasons, and the position of the two ERT lines (blue). Note that only small parts of these trenches have been tested – see Dinnis and French (2023) and references therein for details.

## Results and interpretation

The results of the survey are shown in Figure 3. Although difficult to interpret, they show discrete differences in electrical resistance along the two profiles.

Predicted higher resistance units would be bedrock, coarse rock rubble and dry sediments, while less resistant units (i.e. more conductive units) might consist of clays or water-rich finer grained sediments.

### East-West transect

The eastern end of the east-west transect (Line LR00028, Fig. 3A) exhibits an area of electrically resistant deposits (yellow colour), which corresponds with the uppermost part of an area of known intact sediments (Trench 5: see Dinnis & French 2023). The western end of the section shows the surface of an area of high resistance (yellow/brown), under the cave floor and dipping away from the cave wall. This signal corresponds well with the known surface of the intact Pleistocene deposits in this area, as identified at a depth of c.30-40cm below surface level in the southern part of the excavated area of Trench 9, dipping away from the cave wall (Dinnis & French 2023). Areas of very low resistance (high conductivity; blue) – present near the surface, especially in the middle of the transect – may correspond to near-surface recent disturbance and/or water-saturated sediments. The latter is certainly plausible, given that water consistently pools more in the centre of the cave.

### North-South transect

Highly resistant units (yellow/red) are seen at both ends of the north-south transect (LR00029; Fig. 3B). That at the northern end of the line is likely to be masonry construction of the castle wall, while the highly resistant area at the southern end is possibly bedrock, dipping northwards. Above the latter at the southern end of the line is an area of low resistance (high conductivity; blue). This may be a unit of finer grained sediment (clay?) or water-rich deposits. Two pods of more resistant deposits (yellow/brown) are visible in the profile close to the cave floor. It is noteworthy that the southern part of the more southerly of these two areas lies close to the excavated part of Trench 8 (see Fig. 2), which has been shown to contain several layers of historical-period spoil deposits (Dinnis & French 2023; Dinnis 2023). It is therefore plausible that both of these areas correspond to filled pits.

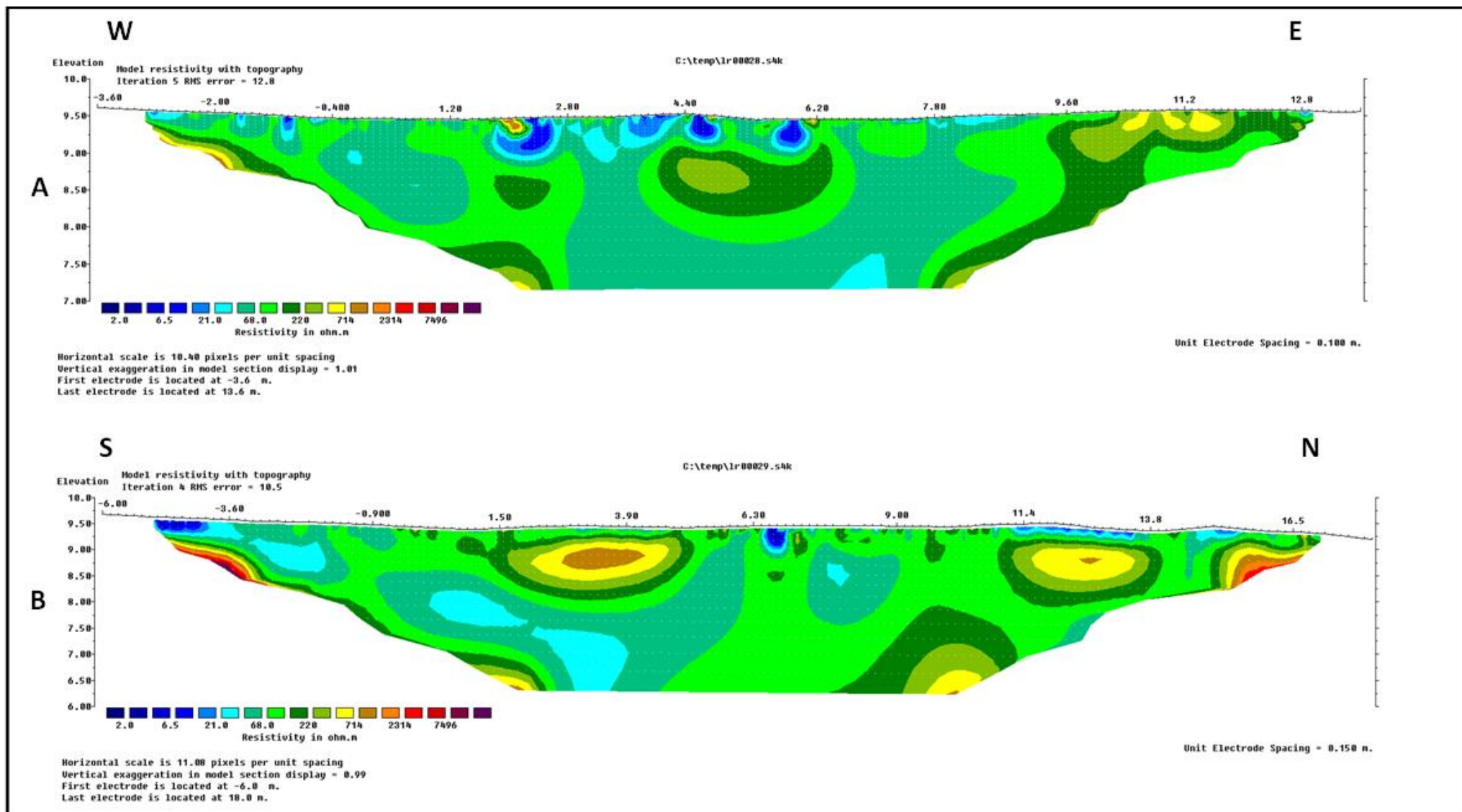


Figure 3: ERT lines LR00028 (A; east-west transect) and LR00029 (B; north-south transect). E = east, N = north etc. Note the lack of data at the ends of the transects reflects the limits of the signal, and not the depth of sedimentary deposits in these areas.

## Concluding comments and future work

Despite being restricted to two transects, the November ERT survey demonstrated clear patterning in resistivity of the deposits at Wogan Cavern. In some cases this patterning can plausibly be related to known or suspected subterranean features or sediment types, demonstrating the overall applicability of the method. Additional geophysical survey work, including further electromagnetics/ERT but also magnetometry and GPR, may therefore help to clarify the nature of the patterning identified here.

## References

Dinnis, R. 2023. *Interim Report on Test Excavations at Wogan Cavern (Pembroke, Pembrokeshire): October 2023 season*. Document prepared for Cadw, November 2023.

Dinnis, R. & French, J. 2023. *Interim Report on Test Excavations at Wogan Cavern (Pembroke, Pembrokeshire): June/July 2023 season*. Document prepared for Cadw, November 2023.

King, D.J.C. 1978. Pembroke Castle. *Archaeologia Cambrensis* 127: 75-121.

Loke, M.H., Acworth, I. & Dahlin, T. 2003. A comparison of smooth and blocky inversion methods in 2D electrical imaging surveys. *Exploration Geophysics* 34: 182-187.

## Appendix 1: ERT transects location data by EDM point ID

<b>LR00028 Line node @ 20cm</b>	<b>X</b>	<b>Y</b>	<b>Z</b>	<b>Direction</b>
168	42.6446	43.0026	9.6141	E-W transect
169	43.457	42.656	9.5689	E-W transect
170	44.4569	42.379	9.5395	E-W transect
171	45.395	42.0464	9.4784	E-W transect
172	46.3275	41.7529	9.4672	E-W transect
173	47.3007	41.4405	9.4558	E-W transect
174	48.2256	41.147	9.4847	E-W transect
175	49.1773	40.8135	9.4928	E-W transect
176	50.1348	40.511	9.5373	E-W transect
177	51.0637	40.2147	9.456	E-W transect
178	52.0398	39.9183	9.4655	E-W transect
179	53.0184	39.6522	9.4654	E-W transect
180	53.9364	39.333	9.5133	E-W transect
181	54.8948	39.0022	9.53	E-W transect
182	55.8491	38.708	9.5754	E-W transect
183	56.7894	38.3786	9.5857	E-W transect
184	57.7552	38.1448	9.5898	E-W transect
185	58.7175	37.9418	9.5542	E-W transect
186	59.2631	37.8534	9.6208	E-W transect
<b>LR00029 Line node @ 30cm</b>	<b>X</b>	<b>Y</b>	<b>Z</b>	<b>Direction</b>
<b>187</b>	44.2223	27.7842	9.69	N-S transect
188	44.5294	28.7504	9.6352	N-S transect
189	44.7572	29.7149	9.6005	N-S transect
190	44.9408	30.6986	9.5522	N-S transect
191	45.1552	31.6791	9.5369	N-S transect
192	45.3576	32.6455	9.492	N-S transect
193	45.6006	33.6131	9.4365	N-S transect
194	45.8228	34.6023	9.3911	N-S transect
195	46.131	35.5725	9.4435	N-S transect
196	46.3083	36.5189	9.472	N-S transect
197	46.5901	37.5033	9.4502	N-S transect
198	46.7957	38.465	9.4292	N-S transect
199	47.0274	39.439	9.4583	N-S transect
200	47.2571	40.4034	9.4763	N-S transect
201	47.4965	41.3797	9.4666	N-S transect
202	47.7495	42.3643	9.4628	N-S transect
203	47.9834	43.3471	9.4427	N-S transect
204	48.1953	44.306	9.5004	N-S transect
205	48.4314	45.2853	9.5085	N-S transect
206	48.6725	46.2759	9.4086	N-S transect
207	48.9423	47.2233	9.3599	N-S transect
208	49.1641	48.1753	9.4568	N-S transect
209	49.4445	49.1294	9.3646	N-S transect
210	49.7038	50.1037	9.328	N-S transect
211	49.9515	51.0658	9.2061	N-S transect